Sterol Carrier Protein-2 Functions in Phosphatidylinositol Transfer and Signaling†

Friedhelm Schroeder,‡ Minglong Zhou,§ Christina L. Swaggerty,§ Barbara P. Atshaves,‡ Anca D. Petrescu,‡ Stephen M. Storey,‡ Gregory G. Martin,‡ Huan Huang,‡ George M. Helmkamp,|| and Judith M. Ball*,§

Department of Physiology and Pharmacology, Texas A&M University, TVMC, College Station, Texas 77843-4466, Department of Pathobiology, Texas A&M University, TVMC, College Station, Texas 77881-4467, and Department of Biochemistry and Molecular Biology, University of Kansas Medical Center, Kansas City, Kansas 66160-7421

Received September 26, 2002; Revised Manuscript Received December 31, 2002

ABSTRACT: Over 20 years ago, it was reported that liver cytosol contains at least two distinct proteins that transfer phosphatidylinositol in vitro, phosphatidylinositol transfer protein (PITP) and a pH 5.1 supernatant fraction containing sterol carrier protein-2 (SCP-2). In contrast to PITP, there has been minimal progress on the structural and functional significance of SCP-2 in phosphatidylinositol transport. As shown herein, highly purified, recombinant SCP-2 stimulated up to 13-fold the rapid (s) transfer of radiolabeled phosphatidylinositol (PI) from microsomal donor membranes to highly curved acceptor membranes. SCP-2 bound to microsomes in vitro and overexpression of SCP-2 in transfected L-cells resulted in the following: (i) redistribution of phosphatidylinositols from intracellular membranes (mitochondria and microsomes) to the plasma membrane; (ii) enhancement of insulin-mediated inositol-triphosphate production; and (iii) 5.5-fold down regulation of PITP. Like PITP, SCP-2 binds two ligands required for vesicle budding from the Golgi, PI, and fatty acyl CoA. Double immunolabeling confocal microscopy showed SCP-2 significantly colocalized with caveolin-1 in the cytoplasm (punctate) and plasma membrane of SCP-2 overexpressing hepatoma cells (72%), HT-29 cells (58%), and SCP-2 overexpressing L-cells (37%). Taken together, these data show for the first time that SCP-2 plays a hitherto unrecognized role in intracellular phosphatidylinositol transfer, distribution, and signaling.

Caveolae are cholesterol-rich, highly curved plasma membrane microdomains that are an entry portal for selective uptake of cholesteryl-esters and HDL-mediated cholesterol trafficking into and out of the cell (*1*, *2*). In addition, caveolae are rich in proteins (reviewed in refs *1* and *3*−*6* and lipids (e.g., phosphatidylinositol (PI),[1] phosphatidylinositol 4-phosphate (PIP), phosphatidylinositol-4, 5-bisphosphate (PIP_2), ceramide, and diacylglycerol)) involved in intracellular vesicular trafficking and/or signaling (reviewed in refs *6*−*9*). Thus, plasma membrane caveolar microdomains are a nexus wherein intracellular lipid transport and signaling pathways meet. However, the mechanism(s) whereby lipids such as cholesterol or PI are transferred between intracellular sites and cell surface membrane caveolae are not completely understood (reviewed in ref *10*).

Recent data suggest that sterol carrier protein-2 (SCP-2) is involved in both vesicular and protein-mediated molecular sterol transfer within the cell (*11*). Although the mechanism whereby SCP-2 participates in vesicular lipid trafficking is unresolved, a number of studies suggest that SCP-2 may mediate the intracellular transfer of PI and participate in PI signaling. Supernatants (pH 5.1) from rat liver and hepatoma cells transfer a broad variety of lipids, including PI, from microsomes in vitro (*12*, *13*). However, the pH 5.1 supernatant is historically the starting fraction for the purification of many lipid transfer proteins, not only SCP-2 but also of phosphatidylinositol transfer protein (PITP) as well as others (*14*). For example, liver fatty acid binding protein (L-FABP) is in the same molecular weight range as SCP-2, is 40−100-fold more prevalent in liver than SCP-2, and exhibits overlapping specificity with SCP-2 for multiple ligands (reviewed in ref *10*) including fatty acyl CoA, a lipid essential for vesicle budding from the golgi (*15*). Thus, one cannot deduce the PI transfer capacity of SCP-2 in the pH 5.1 supernatant fraction in the absence of additional data. Furthermore, SCP-2's potential role in PI transfer was obscured by the concomitant discovery of PITP, now shown to exhibit high affinity for PI, transfer PI, participate in PI signaling, and alter vesicle budding (reviewed in refs *9* and *16*−*19*).

In the present investigation, we hypothesize that SCP-2 may function in PI transfer/metabolism, not only in vitro but also in intact cells. For this hypothesis to be physiologically significant, it is essential for SCP-2 to be localized appropriately within the cell. Analysis of the SCP-2 cDNA

† This work was supported in part by grants from the Texas Advanced Research Program Grant. 0188-97 (J.M.B.), USPHS National Institutes of Health Grant GM63236 (J.M.B.), and the USPHS National Institutes of Health Grant GM31651 (F.S.).

* Corresponding author. Tel: (979) 845-7910. Fax: (979) 845-9231. E-mail: jball@cvm.tamu.edu.

‡ Department of Physiology and Pharmacology, Texas A&M University.

§ Department of Pathobiology, Texas A&M University.

|| University of Kansas Medical Center.

[1] Abbreviations: Fmoc, fluorenylmethoxy-carbonyl; IP_3, inositol-triphosphate; L-FABP, liver fatty acid binding protein; LSCM, laser-scanning confocal microscopy; SUV, small unilamellar vesicles; LUV, large unilamellar vesicles; NBD-stearic acid, (7-nitrobenz-2-oxa-1,3-diazol)-octadecanoic acid; PI, phosphatidylinositol; PIP_2, phosphatidylinositol diphosphate; PITP, phosphatidylinositol transfer protein; POPC, palmitoyloleoyl phosphatidylcholine; SCP-2, sterol carrier protein-2.

10.1021/bi026904+ CCC: $25.00
Published on Web 03/01/2003

sequence reveals the presence of a C-terminal AKL peroxisomal PTS1 targeting sequence, thereby suggesting that SCP-2 might be exclusively peroxisomal (*20*). In contrast, immunogold electron microscopy and immunofluorescence imaging indicate that SCP-2 is present not only in high concentration in peroxisomes, but significant levels of SCP-2 are also present in cytosol, mitochondria, and endoplasmic reticulum (reviewd in refs *20*−*24*). The apparent discrepancy between these experimental and theoretical data was recently resolved by the observation that the gene for SCP-2 actually encodes a precursor protein (pro-SCP-2), which has a 20 residue N-terminal presequence that dramatically affects the secondary and tertiary structure of the protein as well as its targeting (reviewed in refs *20* and *22*). Thus, an adequate concentration of SCP-2 outside the peroxisomes is available for the intracellular transfer of PI.

The purpose of the present investigation was 5-fold: (i) To determine if a highly purified, recombinant human SCP-2 transfers PI from microsomes. (ii) To determine the specificity of SCP-2 in mediating PI transfer as compared to that of other lipid transfer proteins (PITP, L-FABP, BSA) in vitro. (iii) To examine the effect(s) of SCP-2 expression in vivo on the intracellular distribution of PI and on insulin-stimulated PLC activation in transfected cells. (iv) To resolve whether SCP-2 colocalizes with caveolin-1 and/or affects caveolin-1 expression. (v) To determine if SCP-2 and PITP share not just PI as a ligand but also share ligands involved in vesicular trafficking (e.g., fatty acyl CoA).

EXPERIMENTAL PROCEDURES

Materials. Palmitoyloleoyl phosphatidylcholine (POPC) and bovine brain PI were from Avanti (Alabaster, AL). L-3-Phosphatidyl-[2-^{3}H]-inositol was from Amersham Life Science (Arlington Heights, IL). NBD-stearic acid was from Molecular Probes Inc. (Eugene, OR). *Cis*-parinaroyl-CoA was synthesized as described earlier (*25*). Fetal bovine serum (FBS), lithium chloride, and oleoyl CoA were purchased from Sigma Chemical Company (St. Louis, MO). Lab-Tek Coverglass slides were purchased from Fisher Scientific, Pittsburgh, PA. All reagents and solvents used were of the highest grade available and were cell culture tested as necessary.

Proteins. Bovine serum albumin (BSA) was acquired from Sigma Chemical Co. Human recombinant 13.2 kDa SCP-2 (*26*), rat recombinant 14 kDa L-FABP (*27*), and rat recombinant 32 kDa PITPα (*28*) were produced and purified as described. SDS−PAGE followed by silver staining did not detect any significant contaminating proteins (*26*−*28*). PITP was the gift of Dr. George Helmkamp (Department of Biochemistry and Molecular Biology, University of Kansas Medical Center, Kansas City, KS).

Antisera for Western Blotting and Immunolocalization. Mouse monoclonal antibody (IgG_1, clone 5F12) to bovine brain PITP (cross reacts with mouse, rat, and rabbit PITP) was from Upstate Biotechnology (Lake Placid, NY). Rat polyclonal antisera to SCP-2 were prepared according to AAALAC guidelines. Briefly, recombinant SCP-2 (20 μg) was emulsified in Freund's complete adjuvant (200 μL) diluted 1:1 in PBS (200 μL). A pre-bleed was taken prior to injection of the inoculum into a shaved area on the dorsum of male rats (Hazleton Research Products, Denver, PA) as described earlier (*29*). After 6 weeks, a test bleed was taken, and a booster dose (20 μg of SCP-2, 200 μL of Freund's incomplete adjuvant, 200 μL of PBS) was administered. Fourteen days later, the rats were exsanguinated. The resultant polyclonal antibodies were purified by affinity chromatography on protein-A-sepharose. The specificity of appropriate dilutions of the purified anti-SCP-2 antibodies for Western blotting was determined as described earlier (*30*).

For immunolabeling and confocal microscopy of caveolin, L-FABP, and SCP-2, the following antisera were used. Rabbit polyclonal antisera to L-FABP were obtained as described (*31*). Rat polyclonal antisera to SCP-2 were as described above. Polyclonal anti-L-FABP and polyclonal anti-SCP-2 were purified by affinity chromatography on protein-A-sepharose also as described above. Several dilutions (1:20 to 1:200) of the anti-caveolin-1, purified polyclonal anti-SCP-2, and anti-L-FABP antibodies were tested and optimized. Secondary antibodies, goat anti-mouse IgM-Rhodamine Red X antibody, and goat anti-rabbit IgG-FITC were from Jackson Immunoresearch Laboratory (West Grove, PA) and were used at a dilution of 1:100.

Cells. Transfected murine L-cells (arpt$^-$ tk$^-$) overexpressing 15.2 kDa pro-SCP-2 were obtained as described previously (*32*, *33*). SCP-2 expressing and mock-transfected control L-cell fibroblasts were grown to pre-confluence in Higuchi medium supplemented with 10% fetal bovine serum (Hyclone, Logan, UT) (*23*). Mock transfected control and SCP-2 expressing cells expressed 0.007 and 0.030% of cytosolic protein as SCP-2, respectively (*32*, *34*). Mock transfected control and 15.2 kDa pro-SCP-2 transfected McA-RH7777 hepatoma cells were cultured as described (*35*). Western blots of mock transfected McA-RH7777 hepatoma cells detected SCP-2 at levels 10−20-fold lower than liver, while Western blots of SCP-2 overexpressing McA-RH7777 hepatoma cells detected levels similar to liver (*35*). HT-29 cells were cultured as described previously (*36*). Finally, all cells were grown to pre-confluence in their respective media on glass coverslips for immunocytochemistry (*23*).

Peptide Synthesis. A peptide corresponding to the SCP-2 membrane-binding domain (i.e., the first 32 N-terminal residues of SCP-2 (SSASDGFKANLVFKEIEKKLEEEGEQFVKK)) was synthesized and termed $^{1-32}$SCP-2. Fluorenylmethoxy-carbonyl (Fmoc) solid-phase chemistry was used with a Millipore 9050 Plus (Perceptive Biosystems, Foster City, CA) automated peptide synthesizer. The activation chemistry employed was 1-hydroxy-7-azabenzotriazole with diisopropylcarbodiimide. Cleavage of the final peptide product from the solid polymer support and removal of side chain protecting groups was facilitated by the addition of 90% trifluoroacetic acid in the presence of 3% ethanedithiol, 5% thioanisole, and 2% anisole (chemicals from Perceptive Biosystems). Following 2-h incubation, the cleavage mixture containing the cleaved peptide was filtered into a polypropylene tube containing cold diethyl ether (EM Science, Gibbstown, NJ). The peptide was then extracted with cold diethyl ether an additional two times and dried under compressed nitrogen gas prior to the addition of 10% ethanol and lyophilization. Crude peptide was subjected to large scale, gravimetric gel filtration chromatography (Sephadex G25, medium, Sigma Chemical Co.). Peptide peak(s) were detected at 215 nm using an ISCO model 229 UV−vis detector, and fractions corresponding to absorbance peaks

were collected and lyophilized. Further purification was accomplished by reverse-phase HPLC (Beckman, Fullerton, CA) on a C4 column (Waters Corp., Milford, MA). Finally, the peptide was characterized by plasma desorption mass spectrometry (Laboratory for Biological Mass Spectrometry, Texas A&M University).

Phosphatidylinositol Transfer Assay: Preparation of L-3-Phosphatidyl-[2-^{3}H]-inositol Labeled Donor Microsomal Membranes. Microsomes were prepared following an established protocol (*37*) modified as follows: briefly, six rat livers were collected and washed four times with SET buffer (0.25 M sucrose, 1 mM EDTA, and 10 mM Tris-HCl, pH 7.4) at 4 °C. The livers were cut into small pieces, washed once with SET buffer, and then homogenized with a glass grinder on ice. The homogenate was centrifuged at 22 000*g* at 4 °C for 30 min to remove the cell debris. Supernatants were collected, and the microsomes were sedimented at 100 000*g* at 4 °C for 1 h. The microsomal pellet was resuspended in SET buffer, homogenized with a glass grinder, aliquoted, and stored at −80 °C. The protein concentration of the microsome preparation was determined by the BCA protein assay (Pierce, Rockford, IL) as described by the manufacturer following trichloroacetic, ethanol, and acetone extractions.

The microsomal PI pool was labeled by incubation with phosphatidyl-[2-^{3}H]-inositol as described (*37*) with the following modifications: microsomes (20 mg of protein) were sedimented at 100 000*g* at 4 °C for 1 h, resuspended in 2 mL of 50 mM Tris, 2 mM $MnCl_2$ (pH 7.4), and re-homogenized using a glass homogenizer followed by addition of 10 μCi of [2-^{3}H]-inositol. The mixture was incubated at 37 °C for 1.5 h, and then radiolabeled microsomes were sedimented at 100 000*g* for 1 h. To remove unincorporated [2-^{3}H]-inositol, the pellet was resuspended in 10 mM Tris-HCl containing 2 mM inositol (pH 8.6), resedimented at 100 000*g* for 1 h, resuspended again in 30 mL of 1 mM Tris-HCl containing 2 mM inositol (pH 8.6), and resedimented at 100 000*g* for 1 h. The final microsomal pellet enriched in phosphatidyl-[2-^{3}H]-inositol was suspended in 10 mL of SET buffer, aliquoted, and stored at −80 °C.

Phosphatidylinositol Transfer Assay: Preparation of Unlabeled Acceptor Liposomal Membranes. The acceptor liposomes were prepared exactly as previously established (*37*) with the exception that liposomes with low and high surface curvature were utilized. The liposomes containing POPC and PI (molar ratio of 98:2) were extruded through nucleopore filters to make large unilamellar vesicles (LUV, 100−120 nm diameter) or sonicated to produce small unilamellar vesicles (SUV, 20−30 nm diameter) as described (*38*, *39*).

Phosphatidylinositol Transfer Assay: Measurement of Phosphatidyl-[2-^{3}H]-inositol Transfer. Transfer assays were completed essentially as described by Thomas et al. (*37*). The total reaction volume was reduced to 62.5 μL because of the limited source of protein and microsomes. Briefly, the labeled microsomes were pelleted at 100 000*g* at 4 °C for 1 h and resuspended in SET buffer. The protein concentration was adjusted to 1.25 mg/mL and 25 μL of the phosphatidyl-[2-^{3}H]-inositol labeled microsomes were mixed with 25 μL of liposomes. The final ratio of microsomal protein to liposomal lipid in the assay was 1.25 mg of microsomal protein:1 μmol of liposomal lipid (*37*, *40*). To this mixture, 25 μL of the different protein preparations (SCP-2, PITP, and L-FABP) or $^{1-32}$SCP-2 peptide was added to final concentrations as indicated in the figure legends. The mixture was incubated at room temperature for 30 min prior to the addition of 12.5 μL of sodium acetate-sucrose (0.2 M sodium acetate, 0.25 M sucrose) to aggregate the microsomes. The solution was rigorously vortexed and centrifuged at 10 000*g* for 30 min at 4 °C to separate the microsomes from the liposomes. The supernatant containing the liposomes was carefully transferred to a scintillation vial. The microsomal pellet was resuspended in 100 μL of SET buffer and transferred to another scintillation vial. After the addition of 5 mL of scintillation fluid (Cytosin, ICN Biomedicals, Inc. Irvine, CA), the radioactivity was determined with a 1600 TR Tri-Carb liquid scintillation analyzer (Packard Instrument Company, Downers Grove, IL). The percentage of PI transferred was calculated from the radioactivity in the liposomes (supernatant) divided by the total radioactivity.

Subcellular Fractionation for Determination of Intracellular Phosphatidylinositol Distribution. SCP-2 expressing L-cells and mock transfected controls were fractionated to isolate membrane fractions enriched in plasma membranes (*41*), lysosomes (*42*), endoplasmic reticulum (microsomes) (*24*), and mitochondria (*43*). Lipids were extracted from the respective isolated membrane fractions, and phospholipids were resolved by thin-layer chromatography, visualized with iodine vapor, and individual spots scraped, and phospholipid content of each spot was quantitated by phosphate assay as described earlier (*44*).

SCP-2 Binding to Microsomes. Microsomes were isolated as described above to determine if SCP-2 binds to microsomes; 100 μL of microsomes (1.25 mg/mL) were added to a YM100 Microcon filtration unit (molecular mass cutoff 100 kDa) and centrifuged at 7000*g* until all the liquid had passed through the filter. A 200-μL aliquot of SCP-2 (0−54 μg or 0−20 μM) in phosphate buffered saline, pH 7.2 (PBS) was then added to the microsomes, and the microsomes were resuspended and incubated for 30 min at room temperature. Thereafter, the filtration unit was centrifuged as above and washed with an additional 400 μL of PBS and centrifugation at 7000*g* for 30 min. The microsomes were resuspended in 30 μL of 1X SDS−PAGE sample application buffer and transferred to fresh tubes for heating at 100 °C for 5 min. Aliquots of the filtrate were treated similarly. A 5-μL aliquot of microsomes or filtrate in sample application buffer was then loaded to 15% SDS−PAGE gels, electrophoresed, transferred to nitrocellulose, and Western blotted with polyclonal rabbit anti-SCP-2 antisera as described (*30*).

Measurement of Inositol-Triphosphate (IP_3) Production. The effect of SCP-2 expression in L-cells on the production of IP_3 from PIP_2 was measured as described (*45*, *46*). Cells grown to confluency in six well plates were washed with 10 mM lithium chloride (LiCl) for 30 s and incubated in 10 mM LiCl at 37 °C for 7 min to inhibit inositol-1-phosphatase. LiCl was discarded, and cells were treated with either Na-HEPES buffered saline (140 mM NaCl, 4.7 mM KCl, 1.13 mM $MgCl_2$, 10 mM HEPES, 10 mM glucose, 1 mM $CaCl_2$) for background determinations or 10−100 nM insulin from porcine pancreas (Sigma Chemical Co.) for 30 s. Insulin was utilized since L-cells are known to express the insulin receptor (*47*, *48*). Reactions were stopped with 0.2−0.3 volumes of ice cold 20% perchloric acid. Cells were

transferred to a 1.5 mL tube, sonicated for 4 min, incubated on ice for 20 min, and centrifuged at 16 000*g* at 4° for 15 min, and the supernatant was neutralized with 10 M KOH in a new tube. Precipitate was removed by centrifugation, and supernatant was transferred to a siliconized tube for IP_3 analysis by a competitive radioreceptor assay (Amersham Pharmacia Biotech, Piscataway, NJ) according to the manufacturer's instructions. Radioactivity was measured in a 1600 TR Tri-Carb liquid scintillation analyzer (Packard Instrument Company). Standards (0−25 IP_3 pmol/tube) were prepared fresh and used within 1 h. Standard curves were prepared by plotting the percent bound (% B) divided by zero bound (B_0) against the standard concentration on a semilog scale.

Furthermore, the effect of direct addition of SCP-2 on IP_3 production was determined in human, colonic HT-29 cells that express SCP-2 (*36*) using conditions exactly as for L-cells except that that insulin was omitted and either 10 nM neurotensin (known agonist of HT-29 cells), 2 μM L-FABP, or 2 μM SCP-2 were added to stimulate IP_3 production.

Immunolabeling of Cultured Cells for Laser Scanning Confocal Microscopy (LSCM). Mock transfected control and SCP-2 expressing L-cells or hepatoma cells were seeded into two well chamber slides (Nunc, Fisher Scientific, Pittsburgh, PA) and cultured to approximately 80% confluency in Higuchi medium containing 10% FBS (*24*). Cells were washed three times with PBS followed by fixation and permeabilization with cold methanol/acetone (1:1) at −20 °C for 10 min. Nonspecific reactivity was blocked with 2% goat serum-BSA in PBS (pH 7.4, blocking solution) for 1−1.5 h at room temperature or overnight at 4 °C. Mouse anti-caveolin-1 (IgM) diluted at 1:100 and rabbit anti-SCP-2 diluted at 1:50 in blocking solution (0.2 mL) was added to each well and incubated for 1 h. To remove nonspecific antibody binding, cells were washed five times with PBS containing 0.05% Tween-20 over 20−30 min. Secondary antibody (1:100), goat anti-mouse IgM-Rhodamine Red X, and goat anti-rabbit IgG-FITC were reacted for 1 h at room temperature followed by five washes with PBS over 20−30 min. The specificity of immunostaining was established by omitting the primary antibody and using either one or both secondary antibodies, which allowed minimization of nonspecific adsorption of fluorescent antibodies, optimal separation of the fluorescent signals, and optimization of fluorophore concentration to preclude self-quenching (*49*).

HT-29 cells (5×10^3 cells/well) were cultured in eight well chamber slides (Nunc, Fisher Scientific) with DMEM (Sigma Chemical Co), 10% FBS, 1X penicillin/streptomycin, and 1X glutamine overnight (*36*). Medium was removed, and cells were washed three times with calcium-free PBS. After incubation with 0.4 mL of 2 μM SCP-2 or L-FABP for 30 min at 37 °C, cells were fixed in cold methanol/acetone (1:1) for 10 min at −20 °C and sequentially probed with primary antibodies, anti-SCP-2 (1:100), monoclonal IgG mouse anti-caveolin-1 (1:100) (Becton-Dickinson Biosciences, San Diego, CA), and secondary antibodies, goat-anti-rabbit-IgG-Rhodamine Red X (1:100) and goat anti-mouse-IgG-FITC (1:100) (Jackson Immunochemistry Lab., West Grove, PA), for 1 h followed by washing five times with PBS.

To determine whether the SCP-2 taken up by the cells was in vesicles or soluble in the cytoplasm, HT-29 cells in a T75 flask were washed two times with PBS, followed by addition of 5 mL of PBS containing SCP-2 (27 μg/mL, 2 μM). After incubation of cells at 37 °C for 30 min, the cells were washed two times with PBS, treated with 1 mL of 1X trypsin-EDTA (Gibco, Grand Island, NY), transferred to 15-mL conical tubes with 10 mL of PBS, and sedimented at 270*g* for 3 min. The cells were then resuspended in 1.5 mL of phosphate buffered saline, homogenized with a Dounce homogenizer, transferred to 2-mL tubes, and sedimented for 1 h at 56 000 rpm, 4 °C with an RP120AT rotor and RC M120 Centrifuge (Sorvall, Dupont Inc., Wilmington, DE). The pellets were resuspended in 100 μL of 1X SDS−PAGE sample application buffer, loaded onto a 15% SDS−PAGE gel, electrophoresed, transferred to nitrocellulose membranes, and Western blotted with rabbit polyclonal anti-SCP-2 antisera as described earlier (*30*).

Laser Scanning Confocal Microscopy (LSCM). LSCM was performed with a MRC-1024 point scanning laser confocal microscopy system (Bio-Rad, Hercules, CA) equipped with a Zeiss Axiovert 135 inverted microscope, fitted with a 63X, 1.4 N. A. oil immersion lens. FITC or Rhodamine Red X were excited with a 15 mW Kr-Ar laser using the 488 and 568 nm bands, respectively. FITC and Rhodamine Red X emission were detected through a 522/DF35 filter and HQ598/40 band-pass filter, respectively. Confocal images were obtained with Laser Sharp Software (Bio-Rad). Serial horizontal sections (0.3 μm) were taken through the entire thickness of the cell. Figures show single representative horizontal sections.

Image Analysis. Confocal images were processed through Laser Sharp (Bio Rad), MetaMorph (Universal Imaging, The Imaging Division of ASI, Nikon Inc., Melville, NY), Adobe Photo Shop (Adobe Systems Inc., Seattle, WA), and Claris Draw (Apple Computer Inc., Cupertino, CA) software. To obtain a relative quantitative assessment of colocalization of SCP-2 with Caveolin-1, the background fluorescence for each optical section was subtracted, and correlation coefficients were calculated as described earlier (*50*). The data were then fit to a pixel fluorogram (*51*) constructed as described earlier (*50*).

Fatty Acyl CoA and Fatty Acid Binding to PITP. The binding of cis-parinaroyl-CoA to PITP was performed by titrating PITP (127 nM) with increasing *cis*-parinaroyl-CoA (0−1 μM) as described previously (*26*, *52*, *53*). NBD-stearic acid binding to PITP was performed by titrating PITP (127 nM) with increasing NBD-stearic acid (0−1 μM) as described earlier (*54*, *55*). Fatty acyl CoA displacement of PITP-bound NBD-stearic acid was accomplished by preincubating PITP (127 nM) with NBD-stearic acid (1 μM), followed by titration with increasing concentration of oleoyl CoA (0−3 μM) as shown earlier (*26*, *52*, *53*, *55*).

Statistical Analysis. All data were analyzed by one-way ANOVA using Tukey's multiple comparison test. A $p < 0.05$ was considered significant.

RESULTS

Spontaneous Transfer of Phosphatidylinositol from Microsomal Membranes. Spontaneous transfer of PI from microsomal donors to liposomal (SUV) acceptors was determined using a microsome/liposome ratio of 1.25 mg of microsomal protein:1 μmol of liposome lipid as previously established

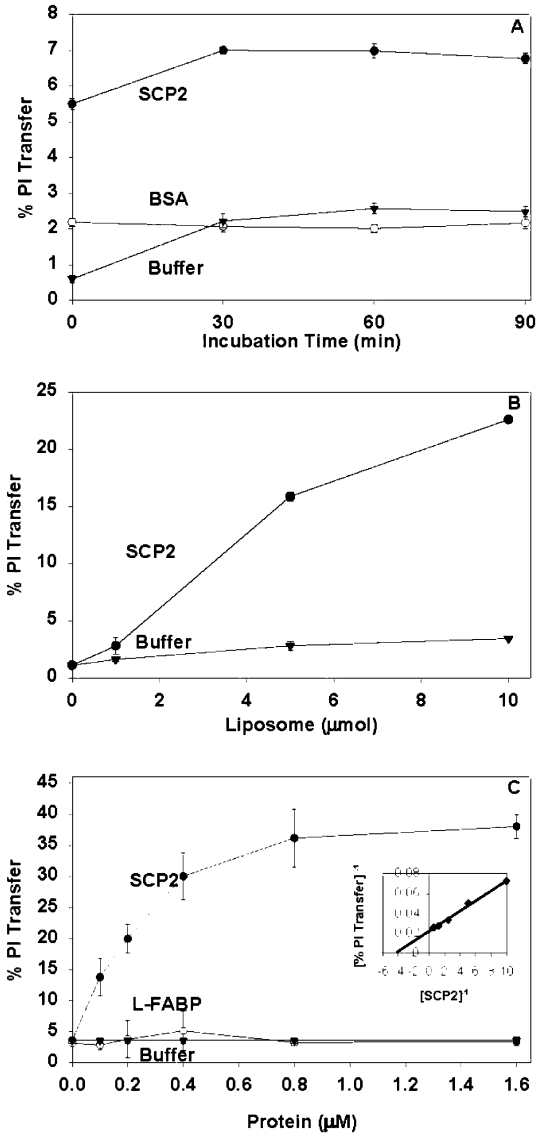

FIGURE 1: SCP-2 functions as a PI transfer protein from microsomes. Values represent the mean ± SD ($n = 6$). PI transfer activity is expressed as % transferred. Panel A: PI transfer was determined from microsomal donors to liposomal SUV acceptors (1.25 mg of protein/mL:1 μM) in the absence of (closed triangles) or presence of 0.4 μM SCP-2 (closed circles) or BSA (open circles). Reactions were stopped after 0, 30, 60, and 90 min incubation. The 0 time point indicates the spontaneous transfer of PI. Panel B illustrates the effect(s) of increasing liposomal (SUV) acceptor concentration on SCP-2 mediated PI transfer. The liposomal SUV concentration was increased from 1 to 10 μM, and PI transfer was measured after 30 min incubation as described in Experimental Procedures. SCP-2 concentration dependence of microsomal PI is depicted in panel C. PI transfer was determined from microsomal donors and liposomal SUV acceptors (1.25 mg of protein/mL:10 μM) after incubation for 30 min in the absence (closed triangles) or presence of SCP-2 (closed circles) or L-FABP (open circles). Protein (SCP-2 or L-FABP) concentrations were varied over the range from 0 to 1.6 μM.

(*40*). Spontaneous PI transfer increased as a function of incubation time at 37 °C (Figure 1A). At time 0 min, 0.55 ± 0.11% of PI was already spontaneously transferred because of the time for mixing and termination of the assay (i.e., 15 s). With increasing incubation time, spontaneous PI transfer increased 4-fold to a maximal value near 2.19 ± 0.14% by 30 min and remained essentially constant over the next 60 min (Figure 1A).

SCP-2 Stimulates Transfer of Phosphatidylinositol from Microsomal Membranes. To resolve the issue of SCP-2 function in PI transfer, the present investigation utilized highly purified, recombinant human SCP-2 shown to be >99% pure by MALDI mass spectrometry as well as SDS−PAGE followed by silver staining (*22*). This allowed direct determination of the concentration dependence in the absence of other contaminating proteins and comparison of the effect of SCP-2 on PI transfer with that of other highly purified lipid-binding proteins (recombinant rat PITP, recombinant rat L-FABP, BSA).

As a function of incubation time, SCP-2 rapidly increased PI transfer. Immediately after addition of SCP-2 (0.4 μM) and mixing (15 s), nearly 5.50 ± 0.15% of PI was already transferred, representing a 10-fold increase over spontaneous PI transfer (Figure 1A, $t = 0$ min). With increasing incubation time, SCP-2 mediated PI transfer increased to a maximal value of 7.00 ± 0.10% by 30 min and remained constant thereafter (Figure 1A). Thus, SCP-2 rapidly (<15 s) enhanced microsomal PI transfer at the earliest measurable time point by nearly 10-fold when compared to spontaneous transfer demonstrating that SCP-2 functions as a PI transfer protein.

As a function of increasing acceptor liposome concentration over a 10-fold range, both the spontaneous and the SCP-2 mediated PI transfer from microsomal donors to liposomal acceptor membranes increased. Spontaneous PI transfer was increased up to 2-fold from 1.70 ± 0.14 to 3.45 ± 0.05% (Figure 1B). Concomitantly, SCP-2 enhanced PI transfer 8.1-fold from 2.80 ± 0.72 to 22.60 ± 0.27% (Figure 1B).

Since these data showed that in the standard PI transfer assay, which utilizes a low molar ratio of microsomal donor/liposome acceptor lipid (*37*), the spontaneous microsomal PI transfer was significantly underestimated by nearly 50%, all subsequent PI transfer assays were performed at the 10-fold higher acceptor liposome levels.

SCP-2 Concentration Dependence of Phosphatidylinositol Transfer from Microsomal Membranes. The SCP-2 concentration dependence of PI transfer from microsomes to liposomes was examined over the range of 0−2 μM SCP-2. With increasing SCP-2, PI transfer from microsomes to liposomes increased 13-fold up to a maximum value of 38.03 ± 1.94% transferred as compared to 3.04 ± 0.44% for spontaneous PI transfer under the same conditions (Figure 1C). The SCP-2 concentration for half-maximal PI transfer was 0.2 μM (Figure 1C). A Lineweaver−Burke plot of these data (Figure 1C, inset) was linear and yielded a K_m near 4.35 μM. Thus, SCP-2 maximally stimulated microsomal PI transfer 13-fold.

Specificity of SCP-2 Mediated Phosphatidylinositol Transfer from Microsomal Membranes. To examine the specificity of SCP-2 mediated PI transfer from microsomes, the effect of equivalent amounts (i.e., 0.4 μM) of two other lipid transfer proteins with broad ligand specificity (BSA and L-FABP) as well as PITP was examined. A concentration of 0.4 μM SCP-2 was chosen since the effect of SCP-2 on PI transfer was not maximal at this concentration (Figure 1C). While 0.4 μM BSA increased the microsomal PI transfer at time 0 slightly at low SUV acceptor concentration, with increasing incubation time 0.4 μM BSA showed no significant effect on PI transfer (Figure 1A). At 10-fold higher SUV

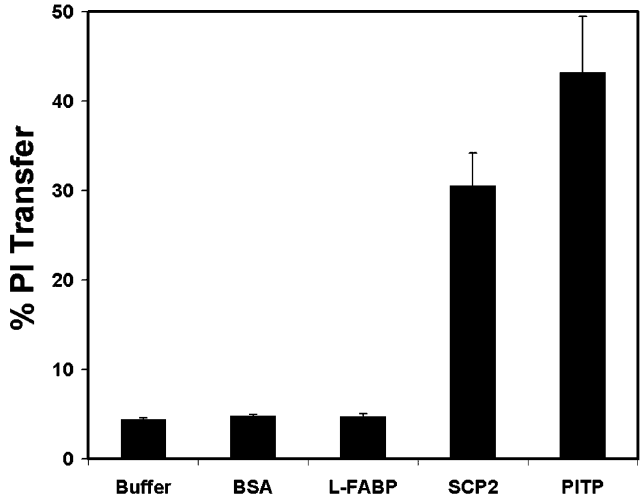

FIGURE 2: Specificity of SCP-2 mediated PI transfer to liposomes (SUV). PI transfer was determined from microsomal donors and liposomal SUV acceptors (1.25 mg of protein/mL:10 μM) after incubation for 30 min in the absence or presence of 0.4 μM SCP-2, PITP, L-FABP, or BSA. PI transfer activity is expressed as % transferred. Values represent the mean $\pm$ SD ($n = 6$).

acceptor concentration, 0.4 μM BSA still did not significantly stimulate microsomal PI transfer (Figures 1B and 2). Similarly, 0.4 μM L-FABP had no effect on microsomal PI transfer (Figure 2), even when the L-FABP concentration was increased 4-fold to 1.6 μM (Figure 1C). In contrast, 0.4 μM PITP increased microsomal PI transfer up to 43.19 $\pm$ 6.26% (Figure 2) as compared to equimolar (0.4 μM) SCP-2 that enhanced microsomal PI transfer to 30.47 $\pm$ 3.72% (Figure 2). In summary, the effect of SCP-2 on microsomal PI transfer was specific and similar to that of PITP under similar conditions, albeit lower.

Interaction of SCP-2 with Microsomal Membranes. To determine if SCP-2 mediated transfer of PI might be mediated, at least in part, by binding to microsomes, microsomes were isolated and incubated with increasing concentrations of SCP-2. The microsomal bound SCP-2 was separated from free SCP-2 by membrane filtration through a 100 kDa molecular weight cutoff filter as described in Experimental Procedures. Purified microsomes did not contain SCP-2 (Figure 3A, lanes 6 and 12). Furthermore, the filter passed free SCP-2 (13 kDa) (Figure 3A, lanes 1 vs 7), but microsomes were excluded as determined by Coomassie staining of SDS−PAGE gels of the filtrates (not shown). Western blotting of the retained microsomes and the filtrate indicated that with increasing SCP-2 concentration, increasing amounts of SCP-2 bound to the microsomes (Figure 3A, lanes 2−5). The total bound (microsomes) and free (filtrate) SCP-2 were determined and shown as a function of increasing SCP-2 concentration added (Figure 3B). At physiological concentrations of SCP-2 (i.e., near 10 μM), approximately one-third of the total SCP-2 added was bound to microsomes under the conditions of the assay.

Role of the SCP-2 Membrane Interaction Domain on Phosphatidylinositol Transfer from Microsomal Membranes. To determine whether SCP-2 interaction with the membranes was, in itself, sufficient to enhance microsomal PI transfer, a synthetic peptide, $^{1-32}$SCP-2, was prepared. The $^{1-32}$SCP-2 peptide is an amphipathic α-helix and comprises the N-terminal membrane-binding domain of SCP-2 (*38*, *39*). However, the $^{1-32}$SCP-2 peptide failed to significantly alter

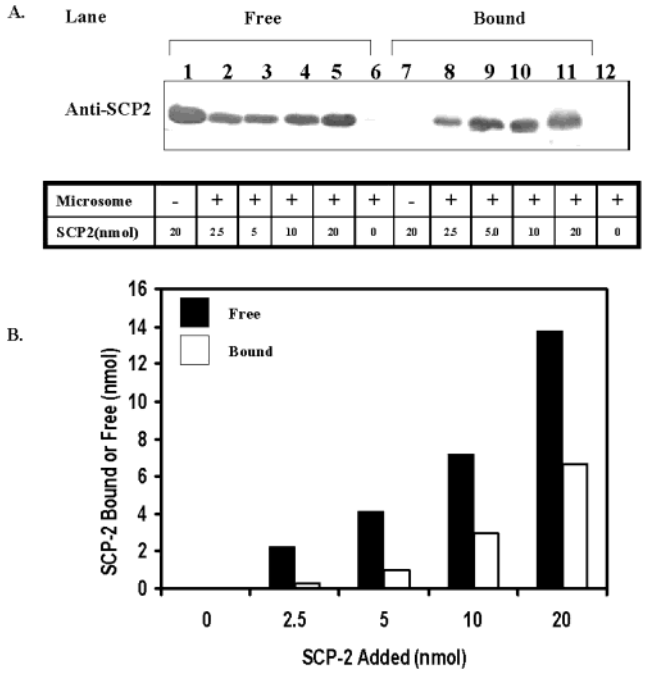

FIGURE 3: SCP-2 interaction with microsomes. Binding of SCP-2 to microsomes was determined with a membrane filtration assay as described in Experimental Procedures. Panel A shows Western blots of aliquots of free SCP-2 in the filtrate (lanes 1−5) and microsome bound SCP-2 (lanes 7−11). The proportions of microsomes and SCP-2 are indicated. Panel B: Total microsome bound and total free SCP-2 were calculated from quantitative analysis of the Western blots in panel A and taking into account the total resuspension volumes of the microsomes and the total volumes of the filtrates.

spontaneous microsomal PI transfer (Figure 4, panel A, 0 μM SCP-2). Likewise, $^{1-32}$SCP-2 peptide did not significantly alter SCP-2-mediated microsomal PI transfer, even when the concentration of $^{1-32}$SCP-2 peptide was 100-fold greater than that of SCP-2 (Figure 4A, 0.4 and 1.6 μM SCP-2). Taken together, $^{1-32}$SCP-2 peptide failed to enhance, potentiate, or inhibit SCP-2 mediated microsomal PI transfer, indicating that the PI transfer function of SCP-2 is not contained in the first 32 residues of SCP2.

Role of Liposome Acceptor Size on Spontaneous and SCP-2 Mediated Phosphatidylinositol Transfer from Microsomal Membrane Donors. To determine the effect of membrane curvature on SCP-2 mediated PI transfer, experiments were performed with acceptor liposomes differing in surface curvature. Liposomes with low surface curvature (LUV) or high surface curvature (SUV) were utilized. Spontaneous PI transfer from microsomal donors to liposomes was not significantly altered by increasing surface curvature (Figure 4B, SUV vs LUV). In contrast, SCP-2 mediated PI transfer was dramatically dependent on liposome surface curvature. SCP-2 enhanced the transfer of microsomal PI to the highly curved SUV by nearly 7-fold, but SCP-2 had no effect on transfer of microsomal PI to the low surface curvature liposomes, LUV (Figure 4B). Since the diameter of SUV used herein was 25 $\pm$ 5 nm while that of LUV was nearly 6-fold greater at 120 $\pm$ 20 nm (*38*), SCP-2 preferentially enhanced the transfer of PI from microsomes to membranes that exhibited high curvature.

Effect of SCP-2 Expression in L-Cells on Intracellular Distribution of Phosphatidylinositol. Since SCP-2 enhanced PI transfer in vitro (Figures 1, 2, and 4), the possibility that

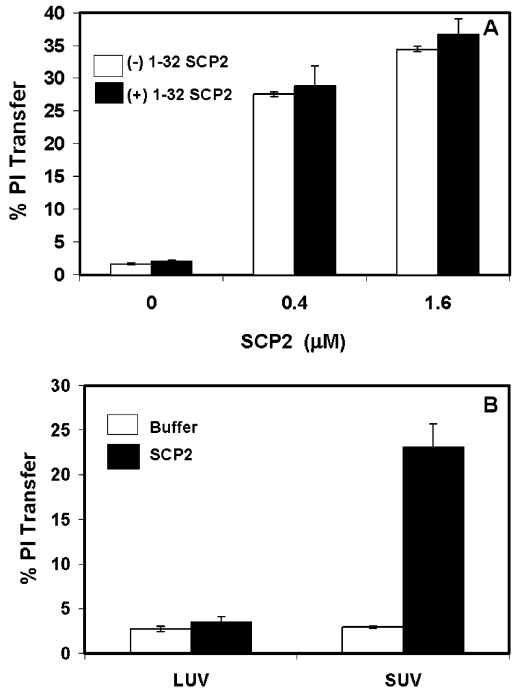

FIGURE 4: Characterization of the PI transfer activity of SCP-2. PI transfer activity is expressed as % transferred. Values represent the mean ± SD (n = 6). Panel A: Effect of $^{1-32}$SCP-2 on spontaneous and SCP-2 mediated microsomal PI transfer. In the absence of SCP-2, PI transfer from microsomal donors and liposomal SUV acceptors (1.25 mg of protein/mL:10 μM) was determined after incubation for 30 min without (open bar) or with (solid bar) 40 mM $^{1-32}$SCP-2. The experiment was repeated in the presence of 0.4 and 1.6 μM SCP-2. Panel B: SCP-2 mediated microsomal PI transfer to liposomes: SUV vs LUV. PI transfer was determined from microsomal donors and liposomal acceptors (1.25 mg of protein/mL:10 μM) after incubation for 30 min in the absence or presence of 0.4 μM SCP-2. Liposomal acceptors were either LUV or SUV as indicated in the abscissa.

SCP-2 may alter the distribution of PI within intact cells was examined. To test this hypothesis, transfected L-cells overexpressing SCP-2 were subjected to subcellular fractionation to obtain fractions enriched in plasma membranes, lysosomal membranes, microsomes, and mitochondria. Analysis of the lipid content of each membrane fraction from control cells revealed that PI mass was highest in mitochondria (81 ± 5 nmol/mg of protein) followed by plasma membranes (41 ± 4 nmol/mg of protein), microsomes (21 ± 2 nmol/mg of protein), and lowest in lysosomal membranes (6.5 ± 3.4 nmol/mg of protein). SCP-2 overexpression in transfected L-cells resulted in significant redistribution of PI among these lipid fractions. PI mass (nmol/mg) was reduced primarily in mitochondria (MITO) and microsomes (ER) by 55 ± 4 and 10 ± 2 nmol/mg ($p < 0.05$), respectively (Figure 5). In contrast, PI mass (nmol/mg of protein) was significantly increased by 13 ± 3 nmol/mg in plasma membrane (PM), while PI mass in lysosomal membranes was essentially unchanged (Figure 5). The same rank order was seen when data were expressed as % change in PI mass in the respective membrane fraction: 68 ± 8% decrease in mitochondria, 48 ± 8% decrease in microsomes, 22 ± 10% decrease in lysosomes, and 31 ± 4% increase in PM (Figure 5). In summary, SCP-2 overexpression significantly redistributed PI from intracellular sources to the plasma membrane.

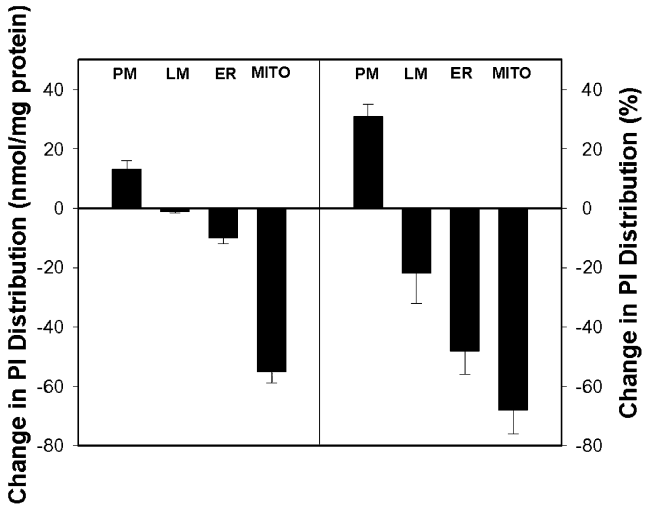

FIGURE 5: SCP-2 expression alters the intracellular distribution of PI. Plasma membranes (PM), ER, lysosomal membranes (LM), and mitochondria (MITO) were isolated from control and SCP-2 expressing cells, followed by lipid extraction and quantitation (nmol/mg) of PI in each fraction. The change in PI distribution in nmol/mg protein (left panel) and in % (right panel) is shown.

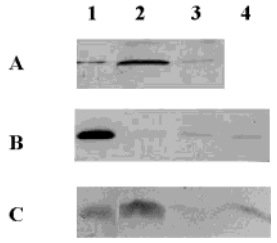

FIGURE 6: Western blot analysis of PITP and SCP-2 in cultured cells. Cell homogenates were subjected to 16% SDS Tricine gel electrophoresis and Western blot using PITP- (panels A and B) and SCP-2-specific (panel C) antibodies. An equivalent amount of protein was added to each lane. Individual lanes in each panel were as follows: panel A was probed with anti-PITP: lane 1, PITP standard; lane 2, mock transfected L-cells; lane 3, SCP-2 overexpressing L-cells. Panel B was probed with anti-PITP: lane 1 PITP standard; lane 2, mock transfected hepatoma cells; lane 3, low SCP-2 overexpressing hepatoma cells; lane 4, high SCP-2 overexpressing hepatoma cells. Panel C was from incubation of HT29 cells with SCP-2, homogenization, and separation of vesicular and soluble SCP-2 as described in Experimental Procedures. The blot was probed with anti-SCP-2: lane 1, cytosol (soluble) fraction from cells incubated in buffer with SCP-2; lane 2, membrane (vesicle) fraction from cells incubated in buffer with SCP-2; lane 3, cytosol (soluble) fraction from cells incubated in buffer without SCP-2; lane 4, membrane (vesicle) fraction from cells incubated in buffer without SCP-2.

Effect of SCP-2 Expression on PITP Level in Transfected Cells. It is possible that the dramatic redistribution of PI from intracellular membranes to plasma membranes of L-cells expressing SCP-2 may not be the result of high SCP-2 levels but of concomitant upregulation of PITP or other protein whose expression is regulated by SCP-2 (e.g., L-FABP) (*56*). However, L-FABP did not enhance transfer of PI (see above). Therefore, the level of PITP was determined by Western blotting in control and SCP-2 expressing cells. Representative Western blots of mock-transfected control L-cells showed that PITP was present at significant levels (Figure 6A, lane 2). Quantitative analysis showed that PITP was expressed as 0.825 ± 0.200 ng/mg of protein in the control L-cells. SCP-2 expression decreased the level of PITP by 5.5-fold to 0.150 ± 0.016 ng/mg of protein (Figure 6A). Thus, PI

Table 1: Effect of SCP-2 and L-FABP on IP_3 Release in Cultured Cells[a]

cell line	peptide/protein added				IP_3 release (fold-increase)
	insulin	neurotensin	L-FABP	SCP-2	
L-cell control	+	−	−	−	1.18 ± 0.04*
L-cell SCP-2 expressor	+	−	−	−	1.25 ± 0.08*
HT-29	−	+	−	−	1.40 ± 0.15*
HT-29	−	−	+	−	0
HT-29	−	−	−	+	1.40 ± 0.14*

[a] The concentrations of peptide or protein added were as follows: 100 nM insulin, 10 nM neurotensin, 0.27 μg of L-FABP, or 0.27 μg of SCP-2. The fold-increase in peptide or protein stimulated IP_3 release above basal (i.e., without peptide or protein) was measured in duplicate and averaged for each of four experiments. An asterisk refers to $p < 0.05$ vs no addition ($n = 4$).

redistribution to the plasma membrane (Figure 5) was not the result of upregulation of PITP. The concomitant down-regulation of PITP upon overexpression of SCP-2 in L-cells was not observed in transfected hepatoma cells overexpressing SCP-2. Western blots of control mock transfected hepatoma cells showed low PITP expression (Figure 6B). Overexpression of SCP-2 at low and high levels in the hepatoma cells did not further decrease the level of PITP, which was unchanged or slightly increased (Figure 6B). In summary, SCP-2 expression in L-cells, but not hepatoma cells, resulted in concomitant down-regulation of PITP. Thus, the effects of SCP-2 expression on PITP level appear to be cell specific.

Effect of SCP-2 on IP_3 Production in L-Cells Overexpressing SCP-2. Since PITP stimulates PI signaling by increasing PIP2 at the plasma membrane for PLC-mediated IP_3 production (*37*), it is anticipated that the down-regulation of PITP would show a decrease in IP_3 production unless PI transfer by SCP-2 compensated for the reduced PITP. Therefore, basal and insulin-stimulated IP_3 levels were monitored in control mock transfected and SCP-2 overexpressing L-cells. Cells were treated with either buffer or insulin for 30 s and assayed for the concentration of IP_3 by a competitive radioreceptor assay. SCP-2 expression had no effect on basal IP_3 release in L-cells (i.e., the buffer treated control and SCP-2 overexpressing cells did not exhibit significantly different background levels of IP_3 production near 30 pmol/tube). In contrast, SCP-2 expression increased insulin-stimulated IP_3 release in L-cells. While low levels of insulin (10 nM insulin, not shown) did not increase IP_3 levels above background in either cell line, 100 nM insulin stimulated IP_3 production by 1.17 ± 0.04 ($n = 4$) and 1.25 ± 0.08-fold ($n = 4$) above basal levels in control and SCP-2 overexpressing cells, respectively (Table 1). Taken together, these data suggested that SCP-2 expression compensated for the loss of PITP in the SCP-2 expressing cells to maintain both basal and insulin stimulated IP_3 production.

Effect of SCP-2 and L-FABP on IP_3 Production in HT-29 Cells. Since SCP-2, but not L-FABP, enhanced PI transfer from microsomal membranes, the ability of SCP-2 and L-FABP to directly enhance IP_3 release was tested under conditions without potential compensatory changes in PITP. HT29 cells were chosen because these cells normally express low levels of the respective proteins as well as PITP (not shown). To ensure that IP_3 production in HT-29 cells was receptor coupled, the HT-29 cells were incubated in the absence or presence of added stimulatory peptide (neurotensin) for 30 s and assayed for the concentration of IP_3 by a competitive radioreceptor assay. As expected, 10 nM neurotensin increased IP_3 production by 1.40 ± 0.15-fold ($n = 4$) above basal levels (Table 1).

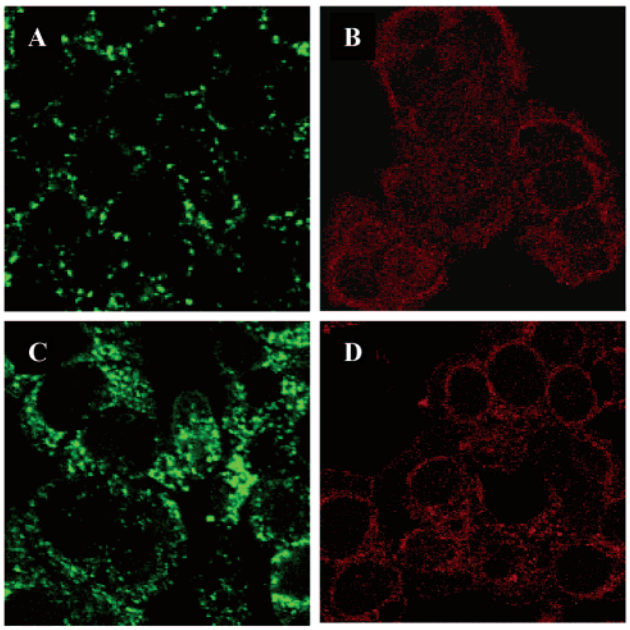

FIGURE 7: Uptake and intracellular distribution of SCP-2 and L-FABP in HT-29 cells. HT-29 cells were incubated with buffer (panels A and B) or buffer containing either 2 μM SCP-2 (panel C) or 2 μM L-FABP (panel D). Cells were then fixed and incubated with primary and secondary antibodies for confocal microscopy as described in Experimental Procedures. Panels A and C were probed with anti-SCP-2 antibodies, while panels B and D were probed with anti-L-FABP antibodies.

To increase the cellular level of SCP-2 or L-FABP, the HT-29 cells were then incubated with buffer alone or with buffer containing either 2 μM SCP-2 or 2 μM L-FABP. To ensure that the cells took up the extracellularly added proteins, intracellular protein levels were monitored. Immunolabeling and confocal microscopy of HT-29 cells incubated with buffer alone detected SCP-2 in a punctate distribution in the cytoplasm (Figure 7A) and L-FABP in a diffuse distribution in the cytoplasm as well as more intensely in the perinuclear region (Figure 7B). Incubation of HT-29 cells with SCP-2 (Figure 7C) or L-FABP (Figure 7D) increased the level of SCP-2 and L-FABP within the cells based on average pixel intensity/cell. The proteins did not accumulate at the cell surface but were taken up and distributed in a similar pattern as in HT-29 cells incubated with buffer alone. Quantitative analysis of multiple cells indicated incubation of HT-29 cells with SCP-2 increased the intensity of SCP-2 detected by 1.6-fold as compared to incubation with buffer alone ($n = 29$, $p < 0.001$). To determine if the SCP-2 taken up was soluble (cytosolic) or vesicular, cells were incubated with or without SCP-2, homogenized, and the soluble and membrane fractions were resolved by ultracentrifugation. For cells incubated with SCP-2, Western blots of equivalent amounts of soluble (Figure 6C, lane 1) and membrane (Figure 6C, lane 2) fractions showed higher levels of SCP-2 in the membrane fraction. When total volumes of the membrane and soluble fraction were taken into account, about 82% of the SCP-2 taken up was soluble, while about

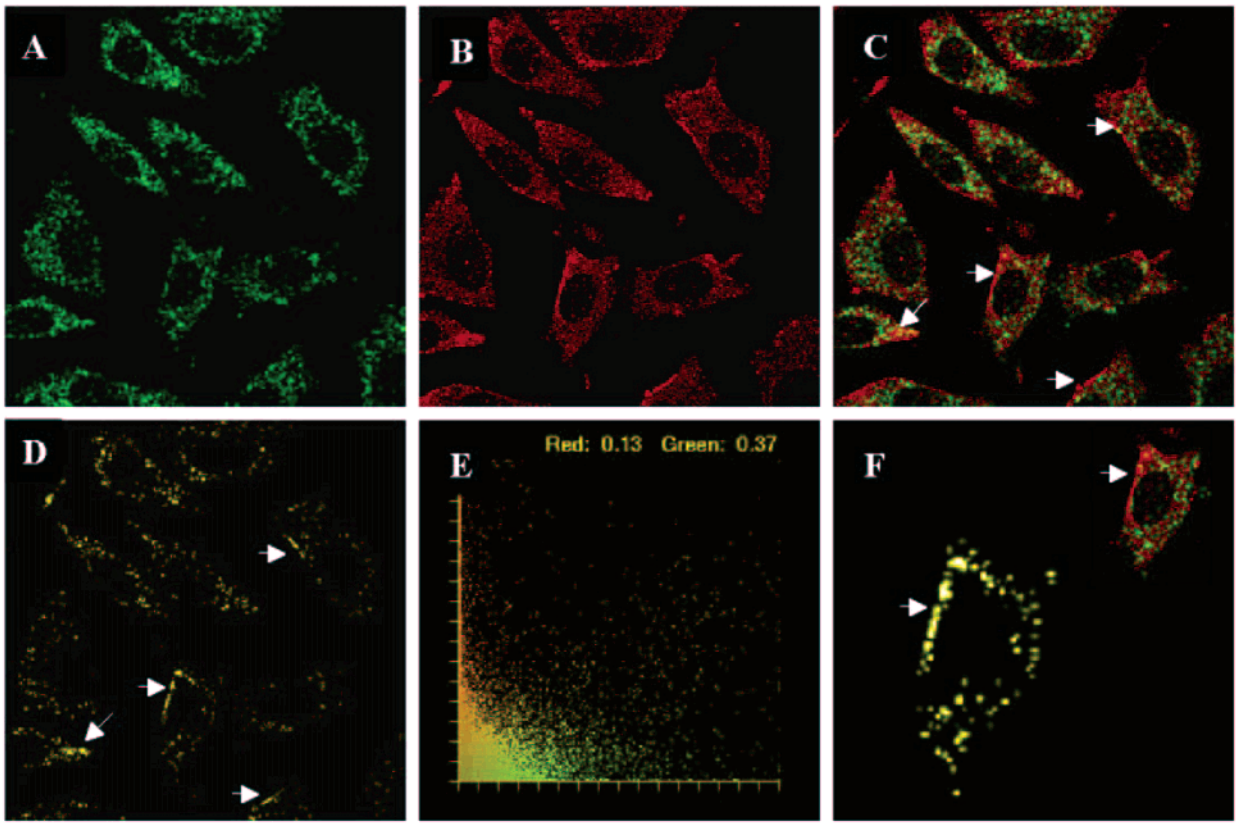

FIGURE 8: Intracellular distribution of SCP-2 and caveolin-1 in SCP-2 expressing L-cells. Cells that overexpress SCP-2 were fixed with methanol/acetone. Caveolin-1 was probed with mouse anti-caveolin-1 (IgM) and goat-anti-mouse IgM-Rhodamine Red X (red), while SCP-2 was probed with rabbit anti-SCP2 and goat anti-rabbit-IgG-FITC (green). Panel A: localization of SCP-2 by laser scanning confocal microscopy, 15 mW Kr-Ar laser with 568 nm band. FITC emission was detected through a 522/DF35 filter. Panel B: localization of caveolin-1 by confocal imaging using a 15 mW Kr-Ar laser with 488 nm band. Rhodamine Red X emission was detected through a HQ598/40 band-pass filter. Panel C: superposition of panels A and B. Panel D: data from panel C in which all noncolocalizing (i.e., separate) red and green pixels were deleted so colocalizing pixels (orange/yellow) can be more readily observed. Panel E: pixel fluorogram of panel C, indicating the ratios of red in green and green in red. Confocal images were processed through the following software packages: Laser Sharp, MetaMorph, Adobe Photo Shop, and Claris Draw. Panel F: magnificationof a typical cell wherein SCP-2 and caveolin-1 were superposed.

18% was membrane (vesicle) associated. In contrast, for cells incubated without SCP-2, the soluble fraction contained no detectable SCP-2 (Figure 6C, lane 3), while the membrane (vesicle) fraction contained barely detectable SCP-2 (Figure 6C, lane 4). Since L-FABP was taken up under the same conditions, basically similar data were obtained for incubation with L-FABP (data not shown).

IP_3 production was then measured in HT-29 cells incubated with buffer alone or with buffer containing added SCP-2, L-FABP, or neurotensin. L-FABP was chosen as a control since it did not affect PI transfer (Figures 1C and 2). Incubation of HT-29 cells with 2 μM SCP-2 enhanced IP_3 release by 1.40 $\pm$ 0.14-fold ($n = 4$) above basal levels similar to that of neurotensin (Table 1). In contrast, incubation of HT-29 cells with 2 μM L-FABP did not significantly affect IP_3 release ($n = 4$) as compared to basal levels (Table 1).

Colocalization of SCP-2 with Caveolin-1: Transfected L-Cell Fibroblasts Overexpressing SCP-2. Transfected L-cells overexpressing SCP-2 were double immunolabeled with anti-sera to SCP-2 (green) and caveolin-1 (red), and simultaneous fluorescence images were obtained by LSCM (Figure 8). SCP-2 was detected primarily in the cytoplasm as punctate structures (Figure 8A, green), with some staining at the plasma membrane. As expected, caveolin-1 was detected throughout the cytoplasm and at the plasma membrane (Figure 8B, red). Superposition of these images showed primarily separate red (caveolin-1) and green (SCP-2) punctate regions (Figure 8C). However, there was extensive colocalization of SCP-2 with caveolin-1 as indicated by orange/yellow pixels within the cytoplasm (Figure 8D, punctate within the cell) and at the plasma membrane (Figure 8D, arrows) when only colocalized pixels were displayed. The latter was shown more clearly in the magnification (Figure 8F, arrow). The region indicated by the arrow in Figure 8F for the single cell demonstrated the colocalization of SCP-2 with caveolin-1 at the plasma membrane in an area especially rich in caveolae. However, as shown in the merged image of this cell (inset of Figure 8F), there was a predominance of red pixels in this region indicating the presence of caveolae not containing SCP-2. A pixel fluorogram of the whole data from the image in Figure 8C showed that 37% of SCP-2 (green fluorescence) colocalized with caveolin-1 (red fluorescence) (Figure 8E). Because of the very low level of SCP-2 in mock-transfected L-cells, it was not possible to acquire accurate colocalization with caveolin therein. These data suggest SCP-2 is structurally localized, at least in part, with plasma membrane regions and vesicles containing caveolin-1 in SCP-2 expressing L-cells.

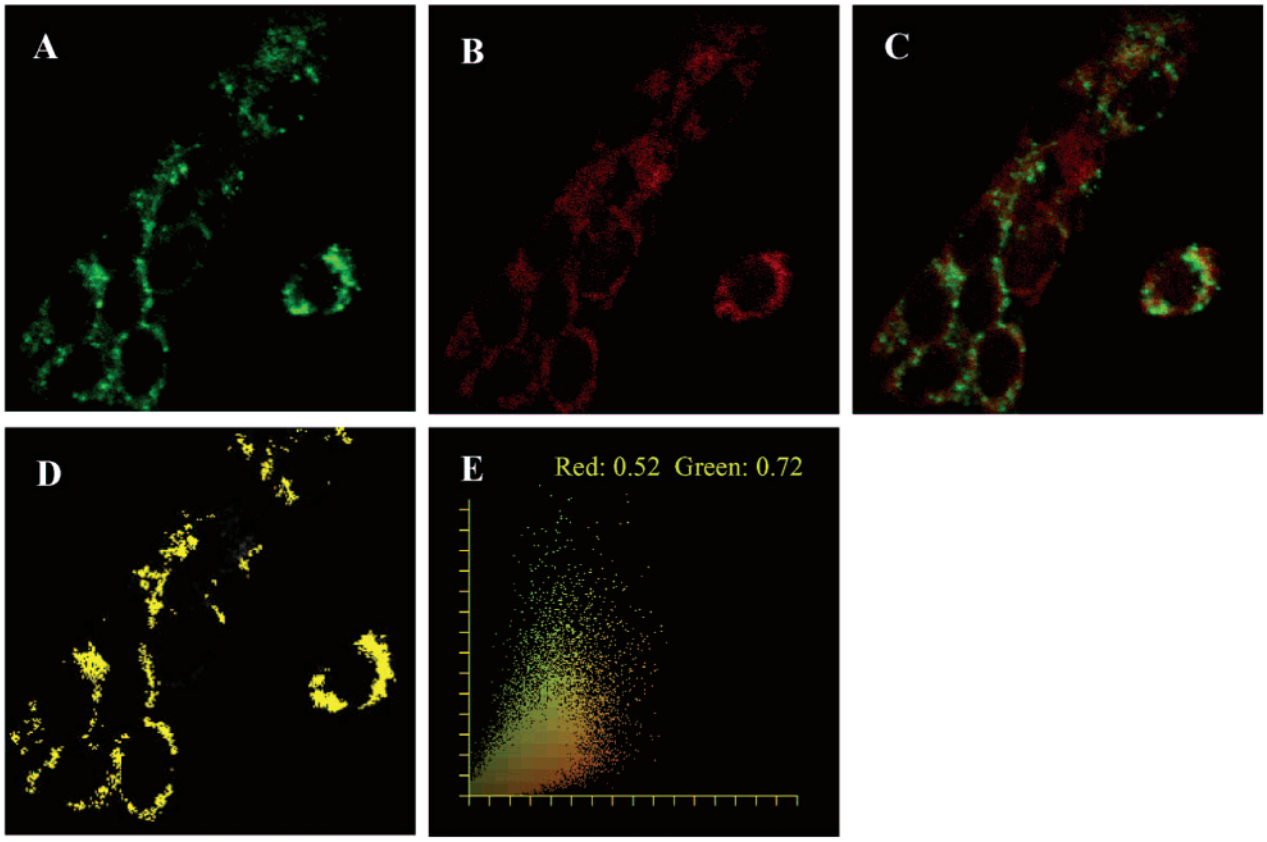

FIGURE 9: Intracellular distribution of SCP-2 and caveolin-1 in SCP-2 expressing hepatoma cells. Hepatoma cells overexpressing SCP-2 were fixed with methanol/acetone. Caveolin-1 was probed with mouse anti-caveolin-1 (IgM) and goat-anti-mouse IgM-Rhodamine Red X (red), while SCP-2 was probed with rabbit anti-SCP2 and goat anti-rabbit-IgG-FITC (green). Panel A: localization of SCP-2. Panel B: localization of caveolin-1. Panel C: superposition of panels A and B. Panel D represents panel C from which all noncolocalizing (i.e., separate) red and green pixels were deleted (i.e., shows only colocalizing yellow/orange pixels). Panel E shows the pixel fluorogram of panel C indicating the ratios of red in green and green in red.

Colocalization of SCP-2 with Caveolin-1: Transfected Hepatoma Cells Overexpressing SCP-2. To determine the extent of SCP-2 colocalization with caveolin-1 at SCP-2 expression levels normally found in liver (*22*, *35*) and other high SCP-2 expressing tissues (reviewed in ref *20*), transfected hepatoma cells overexpressing SCP-2 were double immunolabeled with anti-sera to SCP-2 (green) and caveolin-1 (red) (Figure 9). Simultaneous fluorescence images obtained by LSCM showed SCP-2 was detected as punctuate structures throughout the cell as well as diffusely in the cytoplasm, in the perinuclear region, and less so near the plasma membrane (Figure 9A, green). Immunolabeling and confocal microscopy detected low levels of caveolin-1 distributed primarily throughout the cytoplasm and very little if any at the plasma membrane (Figure 9B, red). Superposition of these images showed many separate green (caveolin-1) and a few separate red (SCP-2) regions (Figure 9C). A significant quantity of SCP-2 colocalized with the low levels of caveolin-1 as indicated by the orange/yellow pixels within the cytoplasm and more intense staining in the perinuclear/golgi region, but there was little colocalization near the plasma membrane (Figure 9C). The latter was shown more clearly when only the orange/yellow pixels were displayed (Figure 9D). A pixel fluorogram of all the pixel data in Figure 9C showed that 72% of SCP-2 (green fluorescence) colocalized with caveolin-1 (red fluorescence) (Figure 9E). In contrast, a pixel fluorogram of mock-transfected control hepatoma cells (10−20-fold lower SCP-2) revealed only 15% of SCP-2 colocalized with caveolin-1 (data not shown), more than 4-fold less than SCP-2 overexpressing hepatoma cells. This SCP-2 concentration dependence of SCP-2/caveolin-1 colocalization was also evident from the nearly 2-fold less SCP-2 colocalization with caveolin in the SCP-2 overexpressing L-cells, which had 2−3-fold lower levels of SCP-2 than the SCP-2 overexpressing hepatoma cells.

Colocalization of SCP-2 with Caveolin-1: HT-29 Cells Normally Expressing SCP-2. To determine the extent of SCP-2 colocalization with caveolin-1 in HT-29 cells, a human cell line that normally expresses low levels of both SCP-2 (Figure 7A) and caveolin-1 (*22*), the HT-29 cells were double immunolabeled with anti-sera to SCP-2 (green) and caveolin (red) (Figure 10). LSCM detected SCP-2 as punctuate structures throughout the cell, in the perinuclear region, and less so near the plasma membrane (Figure 10A, green). Caveolin-1 was distributed primarily in the cytoplasm and somewhat at the plasma membrane (Figure 10B, red). Superposition of the images showed many separate green (caveolin-1) and fewer separate red (SCP-2) regions (Figure 10C). A significant quantity of SCP-2 colocalized with caveolin-1 as shown by orange/ yellow pixels in the cytoplasm, more intensely in the perinuclear/golgi region, and somewhat less near the plasma membrane (Figure 10C). The latter was shown more clearly when only the orange/ yellow pixels were displayed (Figure 10D). A pixel fluorogram (Figure 10E) of the data in Figure 10C showed 58%

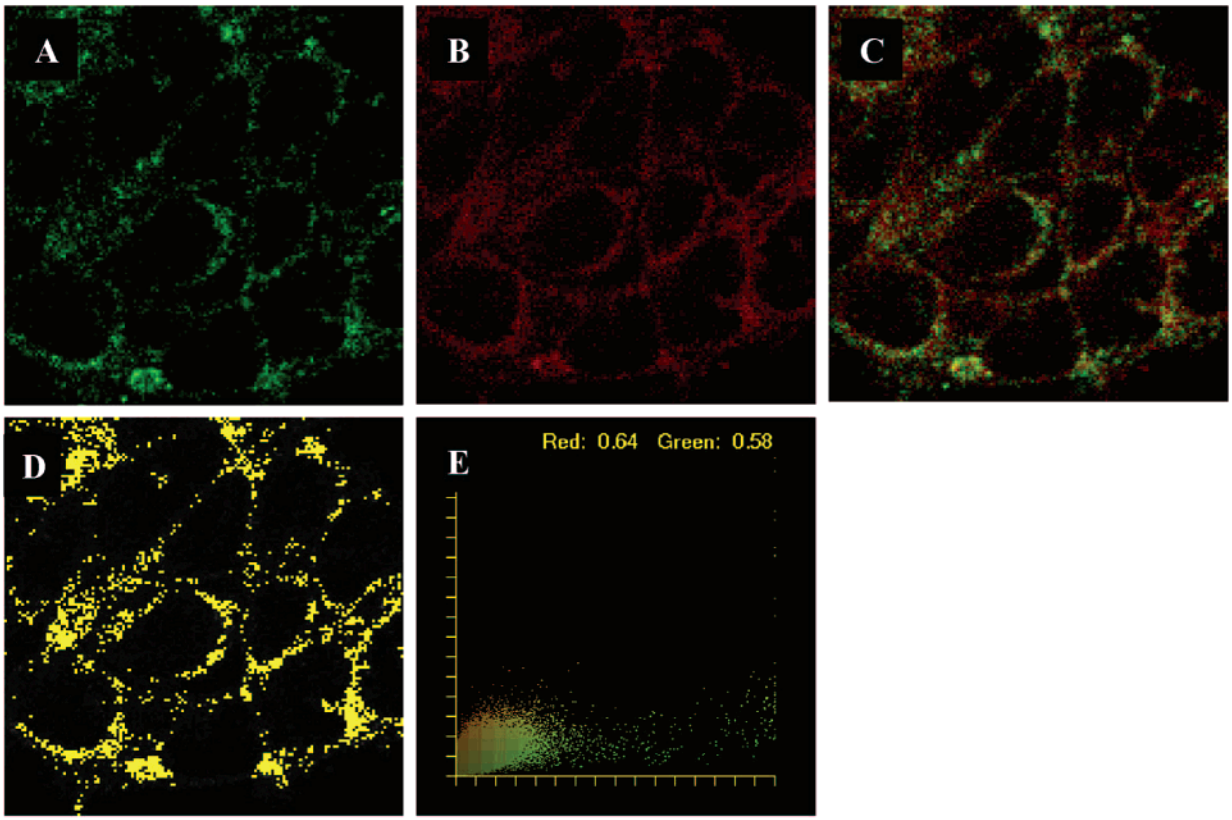

FIGURE 10: Intracellular distribution of SCP-2 and caveolin-1 in HT-29 cells. HT-29 cells were fixed as described in Experimental Procedures. Caveolin-1 was probed with mouse anti-caveolin-1 (IgM) and goat-anti-mouse IgM-Rhodamine Red X (red); SCP-2 was probed with rabbit anti-SCP2 and goat anti-rabbit-IgG-FITC (green) as in Figures 7 and 8. Panel A: localization of SCP-2. Panel B: localization of caveolin-1. Panel C: superposition of panels A and B. Panel D represents panel C from which all noncolocalizing (i.e., separate) red and green pixels were deleted (i.e., shows only colocalizing yellow/orange pixels). Panel E: pixel fluorogram of panel C indicating the ratios of red in green and green in red.

of SCP-2 (green fluorescence) colocalized with caveolin-1 (red fluorescence).

In summary, in three different cell lines (L-cells overexpressing SCP-2, hepatoma cells overexpressing SCP-2, and HT-29 cells) SCP-2 significantly colocalized with caveolin-1.

Specificity of SCP-2 and PITP for Additional Ligands Involved in Vesicular Trafficking. Long chain fatty acids, when metabolically activated to long chain fatty acyl CoAs (*57*), are required for vesicular budding from the golgi (*15*). Although SCP-2 binds both long chain fatty acids (*54*) and long chain fatty acyl CoAs (*26*) with high affinity (nM K_ds), the ability of PITP to share these ligands has not previously been examined.

A fluorescent fatty acid (NBD-stearic acid) binding assay that does not require separation of bound from free ligand showed the fluorescence intensity of NBD-stearic acid (very weak in aqueous buffer, not shown) was dramatically increased in the presence of PITP (Figure 11A). The NBD-binding curve was sigmoidal in shape and resulted in a linear Scatchard plot (Figure 11A, inset) indicating the presence of two binding sites ($n = 2.4$) with similar K_d values of 160 nM. The presence of two fatty acid binding sites was confirmed by Hill plots (not shown), which yielded 1.7 binding sites per molecule of PITP with similar K_d values near 212 nM.

PITP affinity for fatty acyl CoA was determined with a naturally occurring fluorescent fatty acyl CoA (*cis*-parinaroyl CoA) binding assay not requiring separation of bound from free. The fluorescence intensity of *cis*-parinaroyl CoA in aqueous buffer was very weak (not shown) but increased significantly in the presence of PITP (Figure 11B). The concentration dependence of *cis*-parinaroyl CoA binding to PITP yielded a sigmoidal saturation curve (Figure 11B). A Scatchard plot was linear (Figure 11B, inset), consistent with two binding sites ($n = 2$) with similar K_d values of 243 nM. The presence of two *cis*-parinaroyl CoA binding sites was confirmed by a Hill plot of the data (not shown), which yielded 2.1 binding sites per molecule of PITP with similar K_d values near 341 nM. The ability of PITP to bind long chain fatty acyl CoA was confirmed in a fluorescence displacement assay. Increasing concentration of oleoyl-CoA displaced PITP bound NBD-stearic acid (Figure 11C). The K_i for oleoyl CoA displacement of bound NBD-stearic acid was 182 nM. In summary, these data indicate that PITP binds not only PI but also long chain fatty acids and fatty acyl CoAs.

DISCUSSION

Although SCP-2 can transfer lipids (cholesterol, fatty acid, fatty acyl CoA, and phosphatidylcholine) between membranes by molecular transfer (reviewed in refs *10*, *20*, and *58*), it is less clear whether SCP-2 also participates in a meaningful way in phosphatidylinositol trafficking. This is due, at least in part, to the concomitant discovery of PITP, a protein with apparent higher specificity for binding and transferring PI (reviewed in ref *59*). Consequently, PITP has become the focus for its involvement in replenishing PI lost

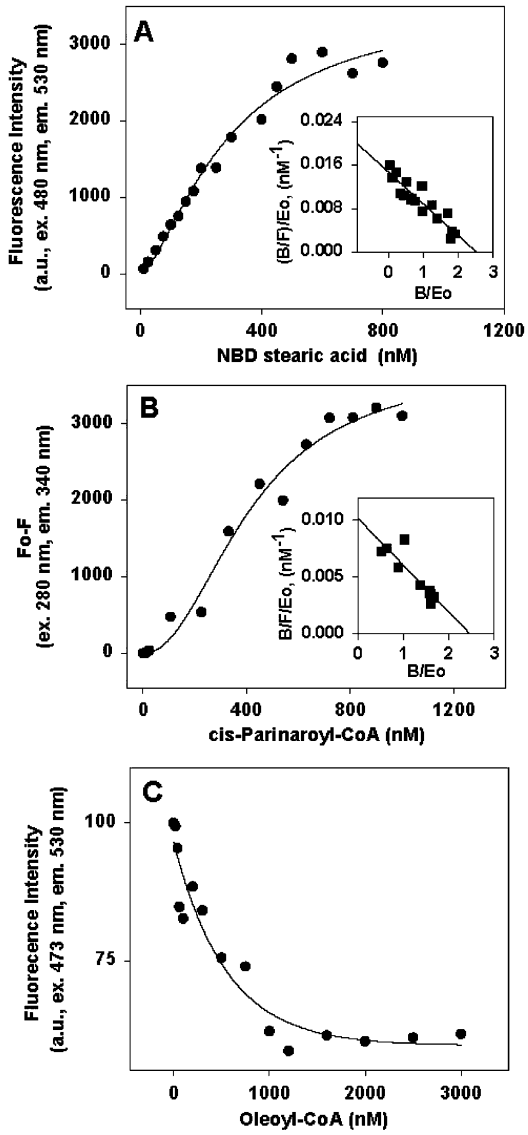

FIGURE 11: PITP binds fatty acids and acyl-CoA thioesters. Panel A: PITP (127 nM) was titrated with NBD-stearic acid (0−1 μM) and excited at 473 nm, and protein-bound NBD-stearic acid was detected as increased fluorescence emission at 530 nm. The inset shows a Scatchard plot of the binding curve as B/F/Eo vs B/Eo, where B is bound ligand in nM, F is free ligand in nM, and Eo is concentration of PITP in nM. The *x* axis intercept indicates the number of binding sites of two ($n = 2.4$) and from the slope a K_d of 239.86 nM was calculated. Panel B: PITP (127 nM) was titrated with cis-parinaroyl-CoA (0−1 μM), and the decrease in protein fluorescence at 340 nm with excitation at 280 nm was measured. The inset shows a Scatchard plot of the same data indicating two binding sites of similar affinities. Panel C: displacement of NBD-stearic acid from PITP by oleoyl-CoA. PITP (127 nM) was first incubated with NBD-stearate (1 μM) and then titrated with oleoyl-CoA (0−3 μM) until no further displacement occurred. From the displacement data, a K_i of 182 nM was calculated for oleoyl-CoA.

to PIP_2 cleavage and IP_3 release, as well as directly providing PI substrates for kinases (reviewed in refs *9*, *17*, *37*, and *60*−*63*). PITP has also been shown to participate in mediating some of the major pathways involved in PI interconversion to produce polyPI signaling molecules essential for vesicle export from the Golgi (reviewed in refs *9*, *17*, *60*, and *62*). In contrast, much less is known regarding potential role(s) of SCP-2 in intracellular PI transfer, signaling, or vesicular trafficking. The work described herein contributes new data indicating SCP-2 also functions in intracellular trafficking of PI.

First, it was demonstrated that highly purified, human recombinant SCP-2 enhanced molecular PI transfer from microsomal (ER) donors to liposomal membranes as much as 13-fold. While such activity had been attributed to SCP-2 present in a crude pH 5.1 supernatant from liver and other tissues (*31*, *39*, *77*−*79*), the present data clearly showed for the first time that a highly purified human recombinant SCP-2 was indeed an effective PI transfer protein in vitro.

Second, the PI transfer activity of SCP-2 from microsomes to liposomal membranes was near that of PITP at equivalent concentration (i.e., 0.4 μM). SCP-2-mediated PI transfer from microsomes to liposomes was only 30% less than that by PITP at equivalent concentration. The 0.4 μM concentration of SCP-2 and PITP used in the microsome to liposome PI transfer assay was in the range of physiological levels that these proteins may achieve in liver cytosol. Although SCP-2 in soluble supernatants of liver homogenates represents 0.08% of soluble protein, or about 10 μM, more than half of this SCP-2 arises from disruption of peroxisomes (wherein SCP-2 is highly concentrated), and much of the remainder is associated with microsomes and mitochondria (reviewed in refs *10* and *20*). Thus, the level of SCP-2 in the cytosol is thought to be less than 1 μM (reviewed in refs *10* and *20*). Densitometric analysis of Western blots of PITP shown for liver soluble proteins (*64*) indicates that PITP represent about 0.02−0.04% of cytosolic protein, near 0.8−1.6 μM. Finally, examination of the linear portion of the PI transfer curve (Figure 1) showed that SCP-2 transferred 38% of microsomal PI/μg of SCP-2 protein added/min to liposomal acceptors. This rate was comparable to PI transfer mediated by PITPβ and 10-fold less than PI transfer mediated by PITPα in an in vitro PI transfer assay between liposomal donors and liposomal acceptors (*28*). It should be noted, however, that the relative ability of PITP as compared to SCP-2 in transferring PI between liposomal donors and liposomal acceptors is highly dependent on the exact lipid composition of both the donor and the acceptor liposomes (not shown).

Third, SCP-2 mediated PI transfer was specific and preferentially transferred to anionic phospholipids in highly curved membranes (SUV) but not to low curvature membranes (LUV). It should be noted that caveolar vesicles contain 50% of total cellular PIP_2, and plasma membrane caveolae are rich in PI (reviewed in refs *1*, *6*, and *19*). The presence of highly anionic phosphoinositides in the cytoplasmic leaflet of caveolar vesicles and spatially segregated, plasma membrane caveolae microdomains induces formation of highly curved membranes, especially in the neck region of caveolae (reviewed in refs *59* and *65*).

Fourth, SCP-2 bound to microsomal membrane PI donors. Although purified microsomal membranes did not contain SCP-2, the SCP-2 significantly bound to microsomal membranes when added in vitro. Immunocytochemistry and confocal microscopy revealed that significant levels of SCP-2 colocalized with endoplasmic reticulum of intact cells (*24*). SCP-2 may bind to membranes by two potential mechanisms: (i) SCP-2 is known to electrostatically bind to anionic phospholipid-containing liposomal membranes (*66*, *67*), and SCP-2 binds to liposomal membranes containing phosphoinositides in the order $PIP_2 > PIP > PI$ (*68*). Examination of

the structure of SCP-2 by NMR (*69*), X-ray crystallography (*70*), circular dichroism (*38*, *39*), and modeling of $^{1-32}$SCP-2 peptide (*38*, *39*) reveals that the SCP-2 N-terminal amphipathic helical region contains positively charged residues clustered on one face of the helix in the SCP-2 protein and $^{1-32}$SCP-2 peptide. The orientation of these positive residues is essential for SCP-2 and $^{1-32}$SCP-2 peptide binding to membranes containing negatively charged phospholipids (*38*, *39*) and for lipid transfer activity of SCP-2 (*38*). (ii) SCP-2 contains pleckstrin homology (PH) domains that recognize and bind PIP_2 (reviewed in refs *71* and *72*). Analysis of the amino acid sequence of SCP-2 (using the program ALIGN, Biology Workbench) revealed 9% identity with PH domains, consistent with sequence similarity of PH domains typically ranging from 10 to 20% (*71*). It is important to note that binding of the amino-terminal SCP-2 peptide ($^{1-32}$SCP-2) did not itself elicit PI transfer (shown herein) or cholesterol transfer (*39*, *73*, *74*).

Fifth, immunofluorescence labeling and LSCM of transfected L- and hepatoma-cells overexpressing SCP-2, as well as HT-29 cells, showed that an extensive amount of SCP-2 (37−72%) was colocalized with caveolin-1. Colocalization was directly related to the level of SCP-2 expression, and colocalization in L-cells occurred both at the plasma membrane and in punctate distribution in the cytoplasm, perhaps reflecting caveolar vesicles or heat shock/caveolin-1/chaperone complexes that represent a small part of intracellular caveolin-1 (*75*).

Sixth, SCP-2 expression in living cells significantly redistributed PI within the cell. Expression of SCP-2 (0.03% of cytosolic protein) at a level similar to that detected in most tissues (0.01−0.08% of cytosolic protein) (reviewed in ref *20*) resulted in a notable decrease of PI mass (nmol/mg of protein) in microsomes and mitochondria, while concomitantly increasing PI content of plasma membranes. This redistribution of PI was not due to upregulation of PITP, the transfer protein generally thought to mediate PI transfer from intracellular sites to the plasma membrane (reviewed in refs *18* and *19*).

Seventh, SCP-2 elicited PLC mediated IP_3 production in intact cells, consistent with the ability of SCP-2 to interact with caveolae at the plasma membrane and play a role in caveolar PI signaling. Although PITP was not detected at the plasma membrane (*76*, *77*), it could still be involved in IP_3 production by promoting PIP2 production through enhancing the resupply of phosphoinositides via the caveolar vesicles released from the Golgi (*60*, *63*, *78*). SCP-2 transfers phosphoinositides in the order PI > PIP > PIP_2 (*68*), while PITP clearly does not transfer polyphosphoinositides (*79*).

In summary, the data presented herein demonstrate a previously unrecognized importance of SCP-2 in PI transfer, in vitro and in intact cells, and in PI intracellular signaling. The fact that SCP-2 and PITP bind both fatty acyl CoA and PI suggests that both proteins may affect vesicle budding from the Golgi and vesicle trafficking from the Golgi through interactions with these ligands (reviewed in ref *59*). The lower affinity of PITP for long chain fatty acyl CoA as compared to that of SCP-2 suggests that PITP may function in initiating vesicular budding from the Golgi cisternae by donating fatty acyl CoA. Another potential function of SCP-2 may be based on the observation of SCP-2-induced PLC-mediated IP_3 production. The production of IP_3 is related not only to phospholipase signaling and vesicular trafficking from the Golgi (*63*) but also to budding of clathrin coated vesicles (transport LDL) from the plasma membrane and subsequent trafficking of LDL lipids via the endosomal pathway to the golgi/lysosomes/ER (reviewed in refs *18* and *19*). Notably, SCP-2 expression enhances cholesterol uptake, the kinetics of which suggest endosomal uptake (*32*). Thus, the overlapping but nonidentical ligand specificities between SCP-2 and PITP together with the different intracellular distributions of these proteins suggests the presence of interrelated pathways whose exact mechanism(s) remain to be explored.

REFERENCES

1. Smart, E. J., and van der Westhuyzen, D. R. (1998) in *Intracellular Cholesterol Trafficking* (Chang, T. Y., and Freeman, D. A., Eds.) pp 253−272, Kluwer Academic Publishers, Boston.
2. Fielding, C. J., Bist, A., and Fielding, P. E. (1998) in *Intracellular Cholesterol Trafficking* (Chang, T. Y., and Freeman, D. A., Eds.) pp 273−288, Kluwer Academic Publishers, Boston.
3. Shaul, P. W., and Anderson, R. G. W. (1998) *Am. J. Phys. 19*, L843−L851.
4. Smart, E. J., Ying, Y., Donzell, W. C., and Anderson, R. G. (1996) *J. Biol. Chem. 271*, 29427−29435.
5. Smart, E. J., Graf, G. A., McNiven, M. A., Sessa, W. C., Engelman, J. A., Scherer, P. E., Okamoto, T., and Lisanti, M. P. (1999) *Mol. Cell. Biol. 19*, 7289−7304.
6. Anderson, R. (1998) *Annu. Rev. Biochem. 67*, 199−225.
7. Anderson, R. G. W. (1993) *Proc. Natl. Acad. Sci. U.S.A. 90*, 10909−10913.
8. Fong, T.-H., and Wang, S. M. (1997) *J. Cell. Biochem. 65*, 67−74.
9. Waugh, M., Lawson, D., Tan, S., and Hsuan, J. J. (1998) *J. Biol. Chem. 273*, 17115−17121.
10. Schroeder, F., Frolov, A., Schoer, J., Gallegos, A., Atshaves, B. P., Stolowich, N. J., Scott, A. I., and Kier, A. B. (1998) in *Intracellular Cholesterol Trafficking* (Chang, T. Y., and Freeman, D. A., Eds.) pp 213−234, Kluwer Academic Publishers, Boston.
11. Atshaves, B. P., Starodub, O., McIntosh, A. L., Roths, J. B., Kier, A. B., and Schroeder, F. (2000) *J. Biol. Chem. 275*, 36852−36861.
12. Bloj, B., and Zilversmit, D. B. (1982) *J. Biol. Chem. 257*, 7608−7614.
13. Fong, T.-H., Wang, S.-M., and Lin, H.-S. (1996) *J. Cell. Biochem. 63*, 366−373.
14. DiCorleto, P. E., Warach, J. B., and Zilversmit, D. B. (1979) *J. Biol. Chem. 254*, 7795−7802.
15. Pfanner, N., Orci, L., Glick, B. S., Amherdt, M., Arden, S. R., Malhotra, V., and Rothman, J. E. (1989) *Cell 59*, 95−102.
16. Wirtz, K. W. A. (1997) *Biochem. J. 324*, 353−360.
17. Fang, M., Rivas, M. P., and Bankaitis, V. A. (1998) *Biochim. Biophys. Acta 1404*, 85−100.
18. Brasaemle, D. L., Levin, D. M., Adler-Wailes, D. C., and Londos, C. (2000) *Biochim. Biophys. Acta 1483*, 251−262.
19. Wang, S.-M., Fong, T.-H., Hsu, S. Y., Chien, C.-L., and Wu, J.-C. (1997) *J. Cell. Biochem. 67*, 84−91.
20. Gallegos, A. M., Atshaves, B. P., Storey, S. M., Starodub, O., Petrescu, A. D., Huang, H., McIntosh, A., Martin, G., Chao, H., Kier, A. B., and Schroeder, F. (2001) *Prog. Lipid Res. 40*, 498−563.
21. Keller, G. A., Scallen, T. J., Clarke, D., Maher, P. A., Krisans, S. K., and Singer, S. J. (1989) *J. Cell Biol. 108*, 1353−1361.
22. Schroeder, F., Frolov, A., Starodub, O., Russell, W., Atshaves, B. P., Petrescu, A. D., Huang, H., Gallegos, A., McIntosh, A., Tahotna, D., Russell, D., Billheimer, J. T., Baum, C. L., and Kier, A. B. (2000) *J. Biol. Chem. 275*, 25547−25555.
23. Atshaves, B. P., Petrescu, A., Starodub, O., Roths, J., Kier, A. B., and Schroeder, F. (1999) *J. Lipid Res. 40*, 610−622.
24. Starodub, O., Jolly, C. A., Atshaves, B. P., Roths, J. B., Murphy, E. J., Kier, A. B., and Schroeder, F. (2000) *Am. J. Physiol. 279*, C1259−C1269.
25. Petrescu, A. D., Hertz, R., Bar-Tana, J., Schroeder, F., and Kier, A. B. (2002) *J. Biol. Chem. 277*, 23988−23999.
26. Frolov, A., Cho, T. H., Billheimer, J. T., and Schroeder, F. (1996) *J. Biol. Chem. 271*, 31878−31884.

27. Jolly, C. A., Wilton, D. A., and Schroeder, F. (2000) *Biochim. Biophys. Acta 1483*, 185−197.
28. Li, H., Tremblay, J. M., Yarbrough, L. R., and Helmkamp, G. M. (2002) *Biochim. Biophys. Acta 1580*, 67−76.
29. Harlow, E. D., and Lane, D. (1988) in *Antibodies, A Laboratory Manual* (Harlow, E. D., and Lane, D., Eds.) Cold Spring Harbor Lab., Cold Spring Harbor, NY.
30. Sambrook, J., Fritsch, E. F., and Maniatis, T. (1989) *Molecular Cloning, A Laboratory Manual*, 2nd ed., Cold Spring Harbor Lab, Cold Spring Harbor, NY.
31. Schroeder, F., Atshaves, B. P., Starodub, O., Boedeker, A. L., Smith, R., Roths, J. B., Foxworth, W. B., and Kier, A. B. (2001) *Mol. Cell. Biochem. 219*, 127−138.
32. Moncecchi, D. M., Murphy, E. J., Prows, D. R., and Schroeder, F. (1996) *Biochim. Biophys. Acta 1302*, 110−116.
33. Murphy, E. J., and Schroeder, F. (1997) *Biochim. Biophys. Acta 1345*, 283−292.
34. Jefferson, J. R., Slotte, J. P., Nemecz, G., Pastuszyn, A., Scallen, T. J., and Schroeder, F. (1991) *J. Biol. Chem. 266*, 5486−5496.
35. Baum, C. L., Reschly, E. J., Gayen, A. K., Groh, M. E., and Schadick, K. (1997) *J. Biol. Chem. 272*, 6490−6498.
36. Swaggerty, C. L., Frolov, A., McArthur, M. J., Cox, V., Tong, S., Compans, R. W., and Ball, J. A. (2000) *Virology 277*, 250−261.
37. Thomas, G. M. H., Cunningham, E., Fensome, A., Ball, A., Totty, N. F., Truong, O., Hsuan, J. J., and Cockcroft, S. (1993) *Cell 74*, 919−928.
38. Huang, H., Ball, J. A., Billheimer, J. T., and Schroeder, F. (1999) *Biochem. J. 344*, 593−603.
39. Huang, H., Ball, J., Billheimer, J., and Schroeder, F. (1999) *Biochemistry 38*, 13231−13243.
40. Basu, J., Kundu, M., Bhattacharya, U., Mazumder, C., and Chakrabarti, P. (1988) *Biochim. Biophys. Acta 959*, 134−142.
41. Jefferson, J. R., Powell, D. M., Rymaszewski, Z., Kukowska-Latallo, J., and Schroeder, F. (1990) *J. Biol. Chem. 265*, 11062−11068.
42. Schoer, J., Gallegos, A., Starodub, O., Petrescu, A., Roths, J. B., Kier, A. B., and Schroeder, F. (2000) *Biochemistry 39*, 7662−7677.
43. Gallegos, A. M., Schoer, J., Starodub, O., Kier, A. B., Billheimer, J. T., and Schroeder, F. (2000) *Chem. Phys. Lipids 105*, 9−29.
44. Murphy, E. J., Stiles, T., and Schroeder, F. (2000) *J. Lipid Res. 41*, 788−796.
45. Dong, Y., Zeng, C. Q. Z., Ball, J. M., Estes, M. K., and Morris, A. P. (1997) *Proc. Natl. Acad. Sci. U.S.A.* 3960−3965.
46. Bozou, J. C., Rochet, N., Magnaldo, I., Vincent, J. P., and Kitabgi, P. (1989) *Biochem. J. 264*, 871−878.
47. Prows, D. R., Jefferson, J. R., Incerpi, S., Heyliger, C. E., Hertelendy, Z. I., Murphy, E., and Schroeder, F. (1993) *FASEB J. 7*, A385.
48. Murphy, E. J., Prows, D. R., Jefferson, J. R., Incerpi, S., Hertelendy, Z. I., Heyliger, C. E., and Schroeder, F. (1996) *Arch. Biochem. Biophys. 335*, 267−272.
49. Musch, A., Cohen, D., and Rodriguez-Boulan, E. (1997) *J. Cell Biol. 138*, 291−306.
50. Manders, E. M. M., Verbeek, F. J., and Aten, J. A. (1993) *J. Microsc. 169*, 375−382.
51. Demandolx, D., and Davoust, J. (1997) *J. Microsc. 185*, 21−36.
52. Frolov, A. A., and Schroeder, F. (1998) *J. Biol. Chem. 273*, 11049−11055.
53. Frolov, A., Cho, T. H., Murphy, E. J., and Schroeder, F. (1997) *Biochemistry 36*, 6545−6555.
54. Schroeder, F., Myers-Payne, S. C., Billheimer, J. T., and Wood, W. G. (1995) *Biochemistry 34*, 11919−11927.
55. Serrero, G., Frolov, A., Schroeder, F., Tanaka, K., and Gelhaar, L. (2000) *Biochim. Biophys. Acta 1488*, 245−254.
56. Seedorf, U., Raabe, M., Ellinghaus, P., Kannenberg, F., Fobker, M., Engel, T., Denis, S., Wouters, F., Wirtz, K. W. A., Wanders, R. J. A., Maeda, N., and Assmann, G. (1998) *Genes Dev. 12*, 1189−1201.
57. Pfanner, N., Glick, B. S., Arden, S. R., and Rothman, J. E. (1990) *J. Cell Biol. 110*, 955−961.
58. Stolowich, N. J., Petrescu, A. D., Huang, H., Martin, G., Scott, A. I., and Schroeder, F. (2002) *Cell. Mol. Life Sci. 59*, 193−212.
59. Szczepaniak, L. S., Babcock, E. E., Schick, F., Dobbins, R. L., Garg, A., Burns, D. K., McGarry, J. D., and Stein, D. T. (1999) *Am. J. Physiol. 276*, E977−E989.
60. Cockcroft, S. (1999) *Chem. Phys. Lipids 98*, 23−33.
61. Cockcroft, S. (1998) *BioEssays 20*, 423−432.
62. Jones, S. M., Alb, J. G., Jr., Phillips, S. E., Bankaitis, V. A., and Howell, K. E. (1998) *J. Biol. Chem. 273*, 10349−10354.
63. Hara, S., Swigart, P., Jones, D., and Cockcroft, S. (1997) *J. Biol. Chem. 272*, 14908−14913.
64. Venuti, S. E., and Helmkamp, G. M. (1988) *Biochim. Biophys. Acta 946*, 119−128.
65. Hooper, N. M. (1999) *Mol. Membr. Biol. 16*, 145−156.
66. Hapala, I., Butko, P., and Schroeder, F. (1990) *Chem. Phys. Lipids 56*, 37−47.
67. Schroeder, F., Butko, P., Hapala, I., and Scallen, T. J. (1990) *Lipids 25*, 669−674.
68. Gadella, T. W., Jr., and Wirtz, K. W. (1991) *Biochim. Biophys. Acta 1070*, 237−245.
69. Garcia, F. L., Szyperski, T., Dyer, J. H., Choinowski, T., Seedorf, U., Hauser, H., and Wuthrich, K. (2000) *J. Mol. Biol. 295*, 595−603.
70. Choinowski, T., Hauser, H., and Piotnek, K. (2000) *Biochemistry 39*, 1897−1902.
71. Perseghin, G., Scifo, P., De Cobelli, F., Pagliato, E., Battezzati, A., Arcelloni, C., Vanzulli, A., Testolin, G., Pozza, G., Del Maschio, A., and Luzi, L. (1999) *Diabetes 48*, 1600−1606.
72. Krssak, M., Petersen, K. F., Dresner, A., DiPietro, L., Vogel, S. M., Rothman, D. L., Shulman, G. I., and Roden, M. (1999) *Diabetologia 42*, 113−116.
73. Huang, H., Gallegos, A., Zhou, M., Ball, J. M., and Schroeder, F. (2002) *Biochemistry 41*, 12149−12162.
74. Seedorf, U., Scheek, S., Engel, T., Steif, C., Hinz, H. J., and Assmann, G. (1994) *J. Biol. Chem. 269*, 2613−2618.
75. Uittenbogaard, A., Ying, Y. S., and Smart, E. J. (1998) *J. Biol. Chem. 273*, 6525−6532.
76. De Vries, K. J., Westerman, J., Bastiaens, P. I., Jovin, T. M., Wirtz, K. W. A., and Snoek, G. T. (1996) *Exp. Cell Res. 227*, 33−39.
77. Jacob, S., Machann, J., Rett, K., Brechtel, K., Volk, A., Renn, W., Maerker, E., Matthaei, S., Schick, F., Claussen, C.-D., and Harring, H.-U. (1999) *Diabetes 48*, 1113−1119.
78. Speed, C. J., and Mitchell, C. A. (2000) *J. Cell Sci. 113*, 2631−2638.
79. Schermoly, and Helmkamp, G. M. (1983) *Brain Res. 268*, 197.

BI026904+